

Moderate hypothermia suppressed excessive generation of superoxide anion radical and inflammatory reactions in blood and liver in heatstroke: Laboratory study in rats

MASAKI TODANI¹, MOTOKI FUJITA¹, RYOSUKE TSURUTA¹, TAKASHI NAKAHARA¹, TAKESHIYAGI¹, CHIYOMI OSHIMA¹, MASATSUGU IGARASHI², KOSHIRO TAKAHASHI², SHUNJI KASAOKA¹, MAKOTO YUASA² & TSUYOSHI MAEKAWA¹

¹Advanced Medical Emergency and Critical Care Center, Yamaguchi University Hospital, Ube, Yamaguchi, Japan, and

²Department of Pure and Applied Chemistry, Faculty of Science and Technology, Tokyo University of Science, Noda, Chiba, Japan

(Received date: 9 December 2009; In revised form date: 28 December 2009)

Abstract

The study was performed to demonstrate superoxide radical ($O_2^{\cdot-}$) generation, systemic inflammation and liver injury caused by heatstroke and to reveal suppressive effects of moderate hypothermia. Heatstroke was defined as achieving pharyngeal temperature of 40°C with arterial pressure reduction. Heatstroke rats were divided to four groups by the temperature after the onset; 40°C, 37°C, 32°C and sham-treated with 37°C. $O_2^{\cdot-}$ current was measured continuously in the right atrium using an electrochemical $O_2^{\cdot-}$ sensor. The $O_2^{\cdot-}$ current increased in all groups except for the sham-treated group during the induction. After the onset of heatstroke, the $O_2^{\cdot-}$ current was suppressed with temperature-dependency. Plasma and liver high-mobility group box 1, intercellular adhesion molecule-1, plasma aspartate aminotransferase and alanine aminotransferase were also suppressed with the suppression of $O_2^{\cdot-}$ generation. Therefore, excessive $O_2^{\cdot-}$ generation might be a key factor in heatstroke and the suppression with moderate hypothermia would be a therapeutic modality.

Keywords: Superoxide, heatstroke, hypothermia, high-mobility group box 1 (HMGB1) protein, malondialdehyde (MDA), intercellular adhesion molecule-1 (ICAM-1)

Introduction

Heatstroke is a life-threatening disease defined as a core temperature rising above 40°C and central nervous system dysfunction including delirium, convulsions or coma [1]. During the 2003 heat wave in France, the mortality in hospital reached 62.6% in spite of intensive care [2]. In heatstroke, ischemic tissue injury and hyperpermeability in the microcirculation occurred because of increased oxygen demand following the inflammation with coagulopathy [3,4]. Multiple organ failure with activated inflammation and coagulopathy is commonly associated with heatstroke. In ischemic status, oxidative stress might be one of the major mechanisms of tissue injury. Oxidative stress is caused by reactive oxygen species (ROS) and reactive nitrogen species

(RNS), including superoxide anion radical ($O_2^{\cdot-}$), hydrogen peroxide (H_2O_2), hydroxyl radical ($OH\cdot$), nitric oxide ($ON\cdot$), alkoxy radical, carbon radical, hydrogen radical, and peroxynitrite ($ONOO\cdot$). In these species, $O_2^{\cdot-}$ is the key radical because many ROS and RNS are derived from $O_2^{\cdot-}$ [5,6]. It is reported that therapeutic hypothermia after the onset of heatstroke suppressed oxidative stress [7,8]. However, the dynamics of $O_2^{\cdot-}$ during heatstroke and therapeutic hypothermia is still unknown.

Recently, we developed an *in vivo* real-time quantitative $O_2^{\cdot-}$ analysis system with an all-synthetic electrochemical $O_2^{\cdot-}$ sensor [9–12]. The current measured by the sensor correlates strongly with the hitting frequency of $O_2^{\cdot-}$ on the surface of the sensor in the circulating blood [11,12].

Correspondence: Motoki Fujita, MD PhD, Advanced Medical Emergency and Critical Care Center, Yamaguchi University Hospital, 1-1-1, Minami-Kogushi, Ube, Yamaguchi 755-8505, Japan. Tel: +81-836-22-2343. Fax: +81-836-22-2344. Email: motoki-ygc@umin.ac.jp

In the present study, we used the $O_2^{\cdot-}$ sensor to measure the dynamics of $O_2^{\cdot-}$ in the mixed venous blood of heatstroke rats and investigated whether $O_2^{\cdot-}$ generation was associated with systemic and liver oxidative stress, endothelial activation, inflammation and liver injury, as evaluated by malondialdehyde (MDA), intercellular adhesion molecule-1 (ICAM-1), high-mobility group box 1 (HMGB1), aspartate aminotransferase (AST), and alanine aminotransferase (ALT). We also investigated the effect of moderate hypothermia after the onset of heatstroke on these parameters in heatstroke rats.

Materials and methods

Experimental animals

This study was approved by the Animal Experiment Committee of Yamaguchi University and was performed in accordance with the guidelines of the United States National Institutes of Health. The experimental protocol is shown in Figure 1. Twenty-eight male Wistar rats (230–280 g) obtained from Japan SLC, Inc. (Shizuoka, Japan) were randomly assigned to four groups: a hyperthermia group (heatstroke rats controlled at 40°C after the onset of heatstroke, $n=7$), a normothermia group (heatstroke rats controlled at 37°C after the onset, $n=7$), a hypothermia group (heatstroke rats controlled at 32°C after the onset, $n=7$) and a sham group (sham-treated rats controlled at 37°C throughout the experiment, $n=7$). Four rats were housed in a cage under controlled temperature ($24 \pm 1^\circ\text{C}$) and humidity conditions with a 12-h light/dark cycle. They were acclimatized to these conditions for 2 weeks prior to the experiment. All rats had access to standard diet and water *ad libitum* the day before the experiment. All animals were disease-free with no signs of systemic inflammation.

Surgical preparation

After overnight fasting, the rats were anaesthetized with 3% isoflurane in O_2 . They were mechanically ventilated (SN-480-7, Shinano Manufacturing Co. Ltd., Tokyo, Japan) through a tracheostomy tube. An arterial catheter was inserted into the left femoral artery to measure mean arterial pressure (MAP) and take blood samples. A venous catheter was inserted to administer drugs through the left femoral vein. The electrochemical $O_2^{\cdot-}$ sensor described in our previous study was inserted from the right external jugular vein and the tip was placed in the right atrium [9–12]. Pancuronium bromide (0.2 mg/h) was given intravenously for mechanical ventilation and heparin (100 U/h intravenously) was given to prevent coagulation on the surface of the $O_2^{\cdot-}$ sensor. Before induction of heatstroke, the core body temperature (T_{core} , measured at the pharynx) of the rats was maintained at $37.0 \pm 0.2^\circ\text{C}$ using a heating pad at room temperature (24°C) and arterial blood pressure and $O_2^{\cdot-}$ current were measured continuously throughout the experiment.

Heatstroke induction and thermal control

After surgery, the anaesthesia was changed to 0.9% isoflurane and 60% N_2 in O_2 . After stabilization of the $O_2^{\cdot-}$ current, the heating pad and an incandescent lamp were used to induce heatstroke by increasing T_{core} to 40°C. T_{core} was elevated by $1.0^\circ\text{C}/10$ min and maintained at 40.0°C . The onset of heatstroke was defined as the moment when the MAP dropped by 10 mmHg from the peak level. After the onset of heatstroke, the incandescent lamp was removed and the heating pad was set to the target temperature for each group. In the hyperthermia group, T_{core} was maintained at 40°C after the onset. In the normothermia and the hypothermia groups, T_{core} was cooled to 37°C and 32°C, respectively,

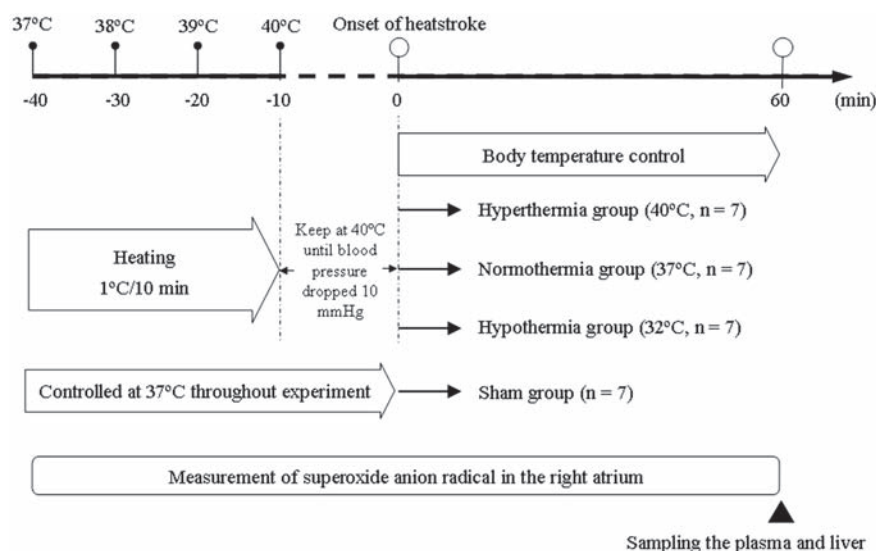


Figure 1. Experimental design.

using a fan, an ice pack, and by spraying alcohol. T_{core} reached the target temperature within 10 min. In the sham group, T_{core} was maintained at 37°C throughout the experiments. All rats were administered normal saline, starting at 10 $\mu\text{l/g/h}$ as a continuous dose after bolus injection of 170 $\mu\text{l/g}$. At 60 min after onset, the blood was sampled and replaced with ice-cold saline. The blood was centrifuged at $900 \times g$ for 10 min at 4°C and the plasma was stored at -80°C until analysis. The liver was removed, frozen in liquid nitrogen and stored at -80°C until analysis.

Mixed venous $\text{O}_2^{\cdot-}$ measurement and evaluation

The $\text{O}_2^{\cdot-}$ generated was measured as a current in the right atrium, which was recorded by an $\text{O}_2^{\cdot-}$ analysis system with an all-synthetic electrochemical $\text{O}_2^{\cdot-}$ sensor (Active Corp., Noda, Japan), as described previously [9–13]. Current data were recorded at two points per second and smoothing procedures (i.e. a moving average) were applied in data analysis [12]. Current data are presented as ΔI , which refers to the difference in current between baseline and the measured current. Baseline current was defined as the stable state before the induction of heatstroke. Measured $\text{O}_2^{\cdot-}$ current was evaluated as the quantified partial value of electricity (Q), which correlates with the

amount of $\text{O}_2^{\cdot-}$ generated [12]. ΔI was integrated before the onset of heatstroke (from the beginning of heat exposure to the onset) as Q_{before} and for 60 min after the onset as Q_{after} .

MDA analysis in plasma and liver

Liver tissue was homogenized in ice-cold 50 mM Tris-HCl buffer (pH 7.4) with 5 mM butylated hydroxytoluene (in acetonitrile) using a Polytron PT-MR3100 homogenizer (Kinematica, Littau, Switzerland). MDA levels in liver homogenate and plasma 60 min after the onset of heatstroke were analysed with a Bioxytech[®] MDA-586[™] kit (Oxis Research[™], Foster, CA). The method is based on the reaction of a chromogenic reagent, N-methyl-2-phenylindole, with MDA at 45°C. The final results are presented as pmol MDA/mg protein in liver homogenate and as μM in plasma. Plasma MDA levels were calculated directly in $\mu\text{g/ml}$.

ICAM-1 analysis in plasma and liver

ICAM-1 levels in liver homogenate and plasma soluble ICAM-1 (sICAM-1) levels 60 min after the onset of heatstroke were analysed with a Quantikine[®] rat sICAM-1 (CD54) Immunoassay[™] kit (R&D

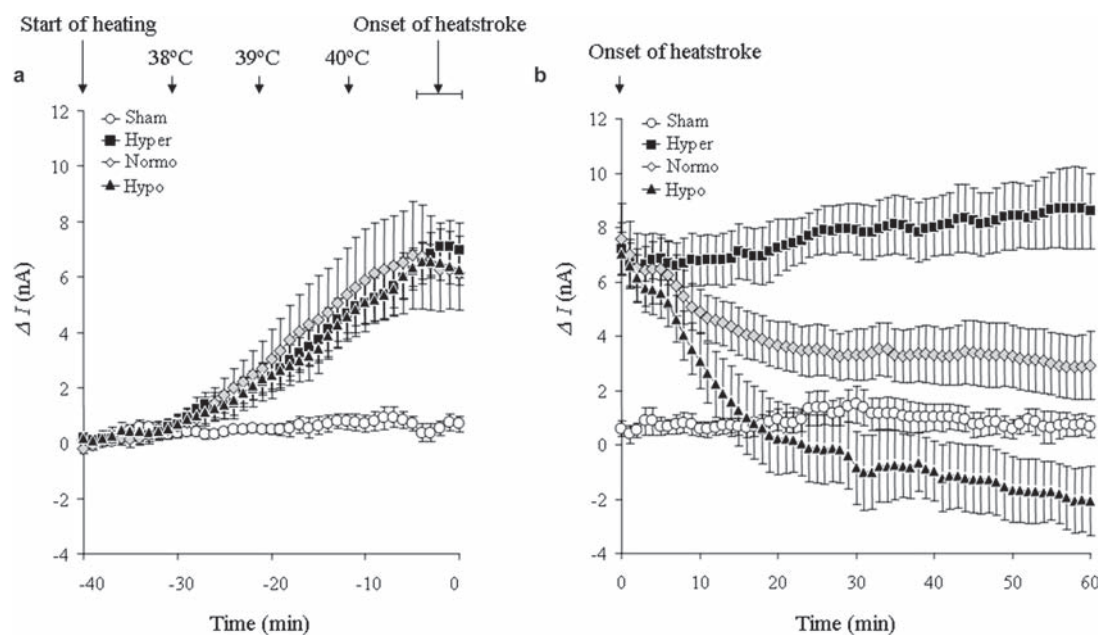


Figure 2. Superoxide anion radical ($\text{O}_2^{\cdot-}$) current during induction and after onset of heatstroke. (a) Change in $\text{O}_2^{\cdot-}$ current during induction of heatstroke. ΔI indicates the difference in the $\text{O}_2^{\cdot-}$ current from baseline, which was defined as the stable state prior to induction. There were significant differences in ΔI between the sham and the hyperthermia groups ($p < 0.05$ at 31, 33 and 34 min; $p < 0.01$ at 35–40 min), the sham and the normothermia groups ($p < 0.05$ at 27–33 min; $p < 0.01$ at 34–40 min), and the sham and the hypothermia groups ($p < 0.05$ at 33 and 34 min; $p < 0.01$ at 35–40 min). Each value is the mean \pm SE of seven measurements. (b) Change in $\text{O}_2^{\cdot-}$ current after the onset of heatstroke. ΔI was significantly higher in the hyperthermia group than that in the sham group ($p < 0.01$ at 0–60 min). ΔI in the normothermia and the hypothermia groups was significantly suppressed compared with that in the hyperthermia group (the hyperthermia group vs the normothermia group, $p < 0.05$ at 22–27, 30–50 min and $p < 0.01$ at 28, 29, 51–60 min; the hyperthermia group vs the hypothermia group, $p < 0.05$ at 10, 11 min and $p < 0.01$ at 12–60 min). Each value is the mean \pm SE of seven measurements. Hyper, the hyperthermia group; Normo, the normothermia group; Hypo, the hypothermia group.

Systems, Inc., Minneapolis, MN). The final results are presented as pg ICAM1/mg protein in liver homogenate and as ng/mL in plasma.

HMGB1 analysis in plasma and liver

The cytoplasmic fraction of liver was prepared as described in our previous report [12]. In brief, liver tissue was gently homogenized in 10 mM N-2-hydroxyethylpiperazine-N'-ethanesulphonic acid/10 mM KCl buffer with 0.08% NP-40, 0.1 mM ethylenediamine tetraacetic acid, 0.5 mM dithiothreitol and 0.5 mM phenylmethylsulphonyl fluoride; the soluble fraction derived from the cytoplasm was kept at -80°C until further testing. HMGB1 levels in liver cytoplasm and plasma 60 min after the onset of heatstroke were analysed with a HMGB1 ELISA Kit IITM (Shino-test Corporation, Kanagawa, Japan). The final results are presented as ng HMGB1/mg protein in liver cytoplasm and as ng/mL in plasma.

AST and ALT analyses

Plasma AST and ALT levels were analysed with the Transaminase CII-test (Wako Pure Chemical Industries, Ltd., Osaka, Japan).

Arterial blood gas and lactate analyses

Blood samples were taken from the femoral arterial catheter before the induction of heatstroke and

60 min after the onset of heatstroke. Arterial blood gas and lactate analyses were performed with the ABL system 555 (Radiometer Medical A/S, Copenhagen, Denmark).

Statistical methods

All data were analysed using the SPSS 10.0 statistical software package (SPSS Inc., Chicago, IL). The statistical significance of ΔI and physiological parameters was determined by two-way analysis of variance (ANOVA). The statistical significance of Q_{before} , Q_{after} , MDA, HMGB1, ICAM-1, AST, ALT, pH, and lactate was determined by one-way ANOVA. When ANOVA was significant, the Bonferroni *post-hoc* test was applied to determine specific group differences. Statistical analyses of the correlation between total Q and MDA, ICAM-1, HMGB1, AST, and ALT were performed using Pearson's correlation coefficient. All data are expressed as the mean \pm standard deviation (SD) of seven measurements, except for ΔI , which is expressed as the mean \pm standard error (SE). Differences were considered to be statistically significant at a value of $p < 0.05$.

Results

Dynamics of mixed venous O_2^- generation and evaluation in heatstroke rats

The mean ΔI of O_2^- in the heatstroke rats before the onset is shown in Figure 2a. When T_{core} was raised

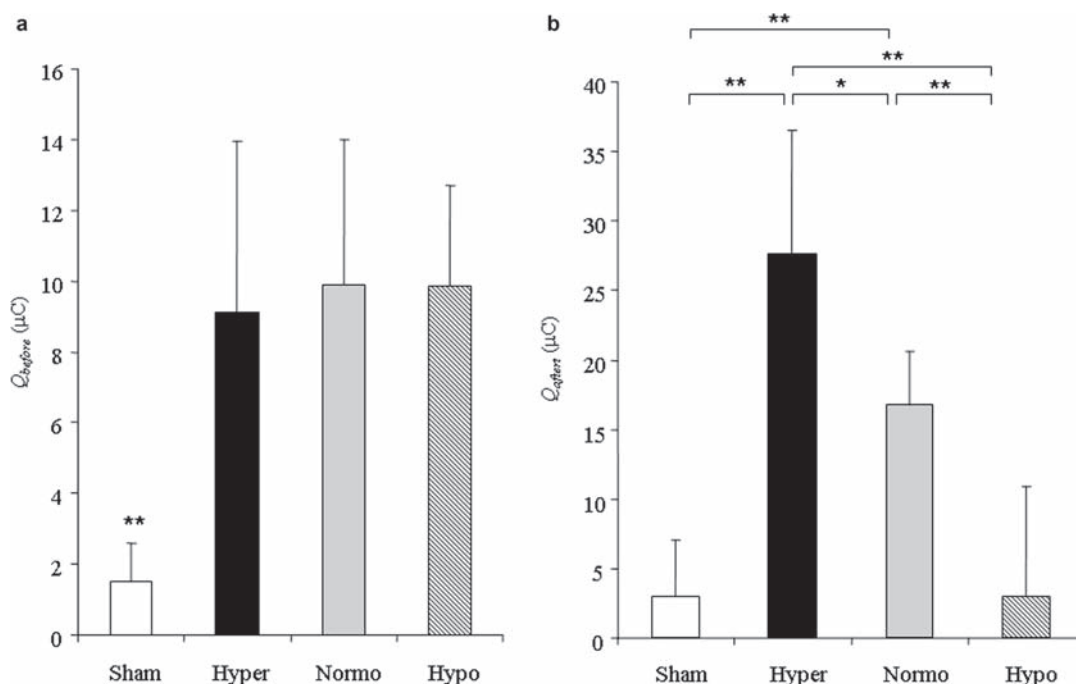


Figure 3. Differences in quantified partial value of electricity (Q) during induction and after onset of heatstroke. (a) Q before the onset of heatstroke (Q_{before}). The generation of O_2^- was evaluated as Q (μC), which was calculated by the integration of ΔI . Each value is the mean \pm SD of seven measurements. $**p < 0.01$ for the sham group vs the hyperthermia, the normothermia and the hypothermia groups. (b) Q after the onset of heatstroke (Q_{after}). Each value is the mean \pm SD of seven measurements. $*p < 0.05$, $**p < 0.01$. Hyper, the hyperthermia group; Normo, the normothermia group; Hypo, the hypothermia group.

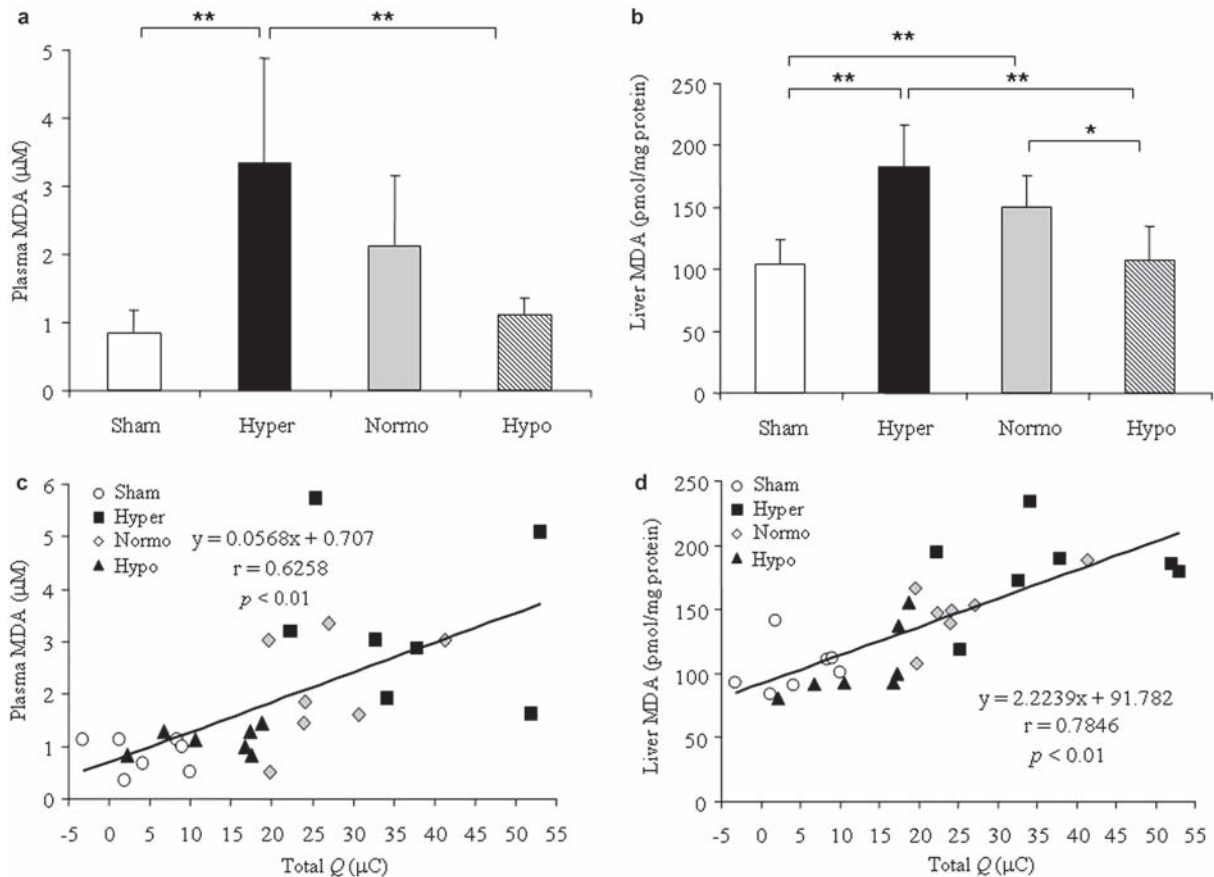


Figure 4. Malondialdehyde (MDA) levels in plasma and liver. (a) MDA in plasma 60 min after the onset of heatstroke. Each value is the mean \pm SD of seven measurements. $**p < 0.01$. (b) MDA in liver tissue 60 min after the onset of heatstroke. Each value is the mean \pm SD of seven measurements. $*p < 0.05$, $**p < 0.01$. (c) Relationship between total Q and plasma MDA. Total Q is the sum of Q_{before} and Q_{after} . (d) Relationship between total Q and liver MDA. Hyper, the hyperthermia group; Normo, the normothermia group; Hypo, the hypothermia group.

to $\sim 38^{\circ}\text{C}$, ΔI began to increase and continued to rise gradually until the onset of heatstroke in the hyperthermia, the normothermia, and the hypothermia groups. There were significant differences in ΔI before the onset between the sham and the hyperthermia groups ($p < 0.05$ at 31, 33 and 34 min; $p < 0.01$ at 35–40 min), the sham and the normothermia groups ($p < 0.05$ at 27–33 min; $p < 0.01$ at 34–40 min) and the sham and the hypothermia groups ($p < 0.05$ at 33 and 34 min; $p < 0.01$ at 35–40 min). There were no significant differences in ΔI among the induced heatstroke groups before the onset of heatstroke.

Mean ΔI after the onset of heatstroke is shown in Figure 2b. After the onset of heatstroke, ΔI began to increase and was significantly higher in the hyperthermia group than that in the sham group ($p < 0.01$ at 0–60 min). In the normothermia group, ΔI decreased after the onset before leveling out above the baseline. In the hypothermia group, ΔI decreased gradually after the onset and was suppressed to levels below the baseline. After the onset, ΔI in the normothermia and the hypothermia groups was significantly suppressed compared with that in the hyperthermia

group (the hyperthermia group vs the normothermia group, $p < 0.05$ at 22–27, 30–50 min and $p < 0.01$ at 28, 29, 51–60 min; the hyperthermia group vs the hypothermia group, $p < 0.05$ at 10, 11 min and $p < 0.01$ at 12–60 min).

We evaluated the amount of $\text{O}_2^{\cdot -}$ generated as Q , which was calculated by the integration of ΔI . Q_{before} and Q_{after} are shown in Figures 3a and b, respectively. Q_{before} in the hyperthermia, the normothermia and the hypothermia groups was significantly higher than that in the sham group ($p < 0.01$ for the sham group vs the hyperthermia, the normothermia, and the hypothermia groups, Figure 3a). Q_{before} was not significantly different among the hyperthermia, the normothermia and the hypothermia groups. Q_{after} was significantly higher in the hyperthermia and the normothermia groups than that in the sham group ($p < 0.01$ for the sham group vs the hyperthermia and the normothermia groups, Figure 3b). Q_{after} in the normothermia and the hypothermia groups was significantly suppressed compared with that in the hyperthermia group ($p < 0.05$ for the hyperthermia group vs the normothermia group; $p < 0.01$ for the hyperthermia group vs the hypothermia group). Q_{after}

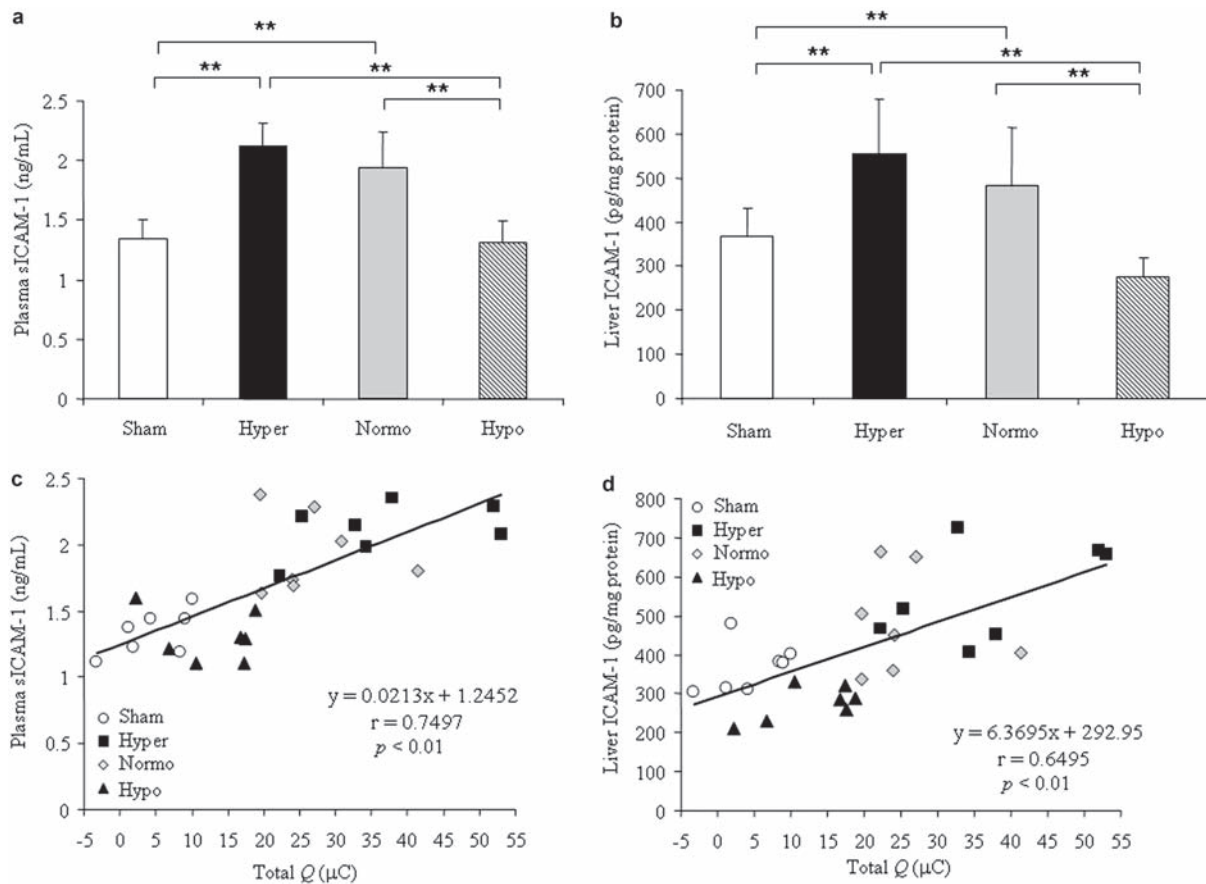


Figure 5. Intercellular adhesion molecule-1 (ICAM-1) concentrations in plasma and liver. (a) Soluble ICAM-1 (sICAM-1) in plasma 60 min after the onset of heatstroke. Each value is the mean \pm SD of seven measurements. $**p < 0.01$. (b) ICAM-1 in liver tissue 60 min after the onset of heatstroke. Each value is the mean \pm SD of seven measurements. $**p < 0.01$. (c) Relationship between total Q and plasma sICAM-1. Total Q is the sum of Q_{before} and Q_{after} . (d) Relationship between total Q and liver ICAM-1. Hyper, the hyperthermia group; Normo, the normothermia group; Hypo, the hypothermia group.

in the hypothermia group was significantly suppressed compared with that in the normothermia group ($p < 0.01$). We found that a reduction in T_{core} corresponded to a decrease in Q_{after} .

Plasma and liver MDA in heatstroke rats

Levels of plasma and liver MDA 60 min after the onset of heatstroke are shown in Figures 4a and b, respectively. All plasma and liver MDA values tended to increase with increasing T_{core} after the onset. Except for plasma MDA in the normothermia group, values in the hyperthermia and the normothermia groups were significantly higher than those in the sham group ($p < 0.01$ for the sham group vs the hyperthermia and the normothermia groups). Values in the hypothermia group were significantly suppressed compared with those in the hyperthermia group ($p < 0.01$ for the hyperthermia group vs the hypothermia group).

For each of the four groups, correlation coefficients were calculated between total Q (equal to $Q_{\text{before}} + Q_{\text{after}}$) and plasma MDA and between total Q and liver MDA to test for a correlation between mixed venous O_2^- generation and the degree of lipid

peroxidation in plasma and liver. Total Q was significantly correlated with plasma MDA ($r = 0.6258$, $p < 0.01$, Figure 4c) and liver MDA ($r = 0.7846$, $p < 0.01$, Figure 4d).

Plasma sICAM-1 and liver ICAM-1 in heatstroke rats

Levels of plasma sICAM-1 and liver ICAM-1 60 min after the onset of heatstroke are shown in Figures 5a and b, respectively. Plasma sICAM-1 and liver ICAM-1 in the hyperthermia and the normothermia groups were significantly higher than those in the sham group ($p < 0.01$ for the sham group vs the hyperthermia and the normothermia groups). Levels in the hypothermia group were significantly suppressed compared with those in the hyperthermia and the normothermia groups ($p < 0.01$ for the hypothermia group vs the hyperthermia and the normothermia groups).

For the four groups, we calculated the correlation coefficients between total Q and plasma sICAM-1 and between total Q and liver ICAM-1. Total Q was significantly correlated with plasma sICAM-1 ($r = 0.7497$, $p < 0.01$, Figure 5c) and liver ICAM-1 ($r = 0.6495$, $p < 0.01$, Figure 5d).

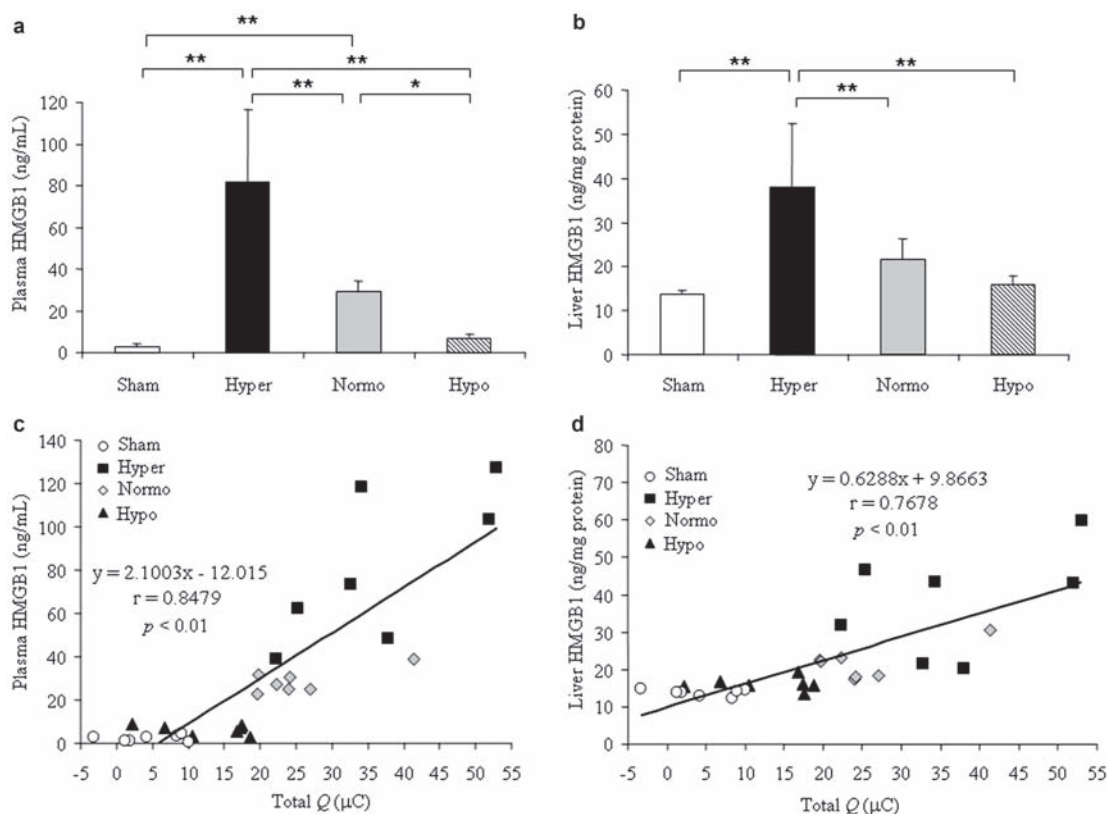


Figure 6. High mobility group box 1 (HMGB1) concentrations in plasma and cytoplasm of liver tissue. (a) HMGB1 in plasma 60 min after the onset of heatstroke. Each value is the mean \pm SD of seven measurements. * $p < 0.05$, ** $p < 0.01$. (b) HMGB1 in liver cytoplasm 60 min after the onset of heatstroke. Each value is the mean \pm SD of seven measurements. ** $p < 0.01$. (c) Relationship between total Q and plasma HMGB1. Total Q is the sum of Q_{before} and Q_{after} . (d) Relationship between total Q and liver HMGB1. Hyper, the hyperthermia group; Normo, the normothermia group; Hypo, the hypothermia group.

Plasma and liver HMGB1 in heatstroke rats

Levels of plasma and liver HMGB1 60 min after the onset of heatstroke are shown in Figures 6a and b, respectively. Except for liver HMGB1 in the normothermia group, all values for plasma and liver HMGB1 were significantly higher in the hyperthermia and the normothermia groups than those in the sham group ($p < 0.01$ for the sham group vs the hyperthermia and the normothermia groups, Figures 6a and b). Except for liver HMGB1 in the normothermia group, values of plasma HMGB1 and liver HMGB1 were significantly suppressed in the hypothermia group compared with the hyperthermia and the normothermia groups ($p < 0.05$ for plasma HMGB1 in the normothermia group vs the hypothermia group; $p < 0.01$ for plasma and liver HMGB1 in the hyperthermia group vs the hypothermia group). Plasma HMGB1 was significantly suppressed in the normothermia group compared with that in the hyperthermia group ($p < 0.01$).

For the four groups, we calculated the correlation coefficients between total Q and plasma HMGB1 and between total Q and liver HMGB1. Total Q correlated significantly with plasma HMGB1 ($r = 0.8479$, $p < 0.01$, Figure 6c) and with liver HMGB1 ($r = 0.7651$, $p < 0.01$, Figure 6d).

Plasma AST and ALT in heatstroke rats

Plasma AST and ALT values 60 min after the onset of heatstroke are shown in Figures 7a and b, respectively. AST and ALT were significantly higher in the hyperthermia group than that in the sham group ($p < 0.01$). Total Q correlated significantly with AST ($r = 0.6233$, $p < 0.01$, Figure 7c) and with ALT ($r = 0.6154$, $p < 0.01$, Figure 7d).

Physiological parameters in heatstroke rats

Levels of MAP during the experiments are shown in Figure 8a. MAP was lower in the hyperthermia group than that in the sham group from 30–60 min after the onset of heatstroke ($p < 0.01$ for the sham group vs the hyperthermia group). There was a greater degree of lactic acidosis in the hyperthermia and the normothermia groups than that in the sham group ($p < 0.01$ for the sham group vs the hyperthermia and the normothermia groups, Figures 8b and c). Lactic acidosis was significantly suppressed in the hypothermia group compared with that in the hyperthermia and the normothermia groups.

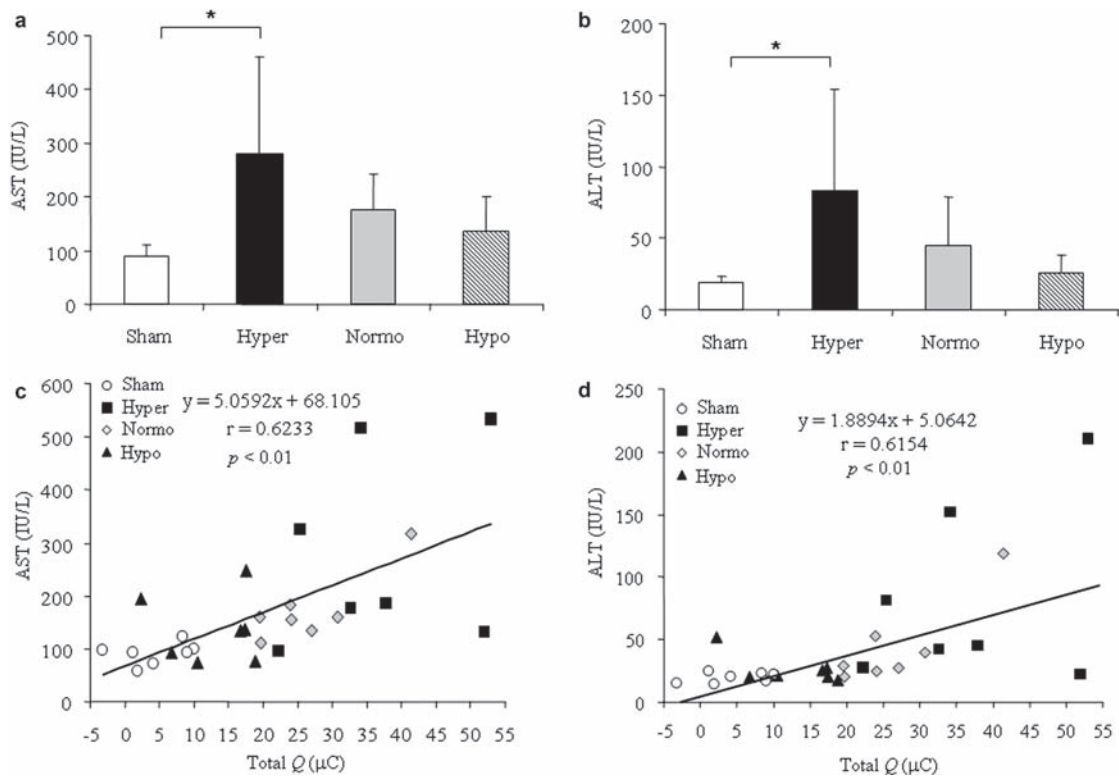


Figure 7. Aspartate aminotransferase (AST) and alanine aminotransferase (ALT) in plasma. (a) AST in plasma 60 min after the onset of heatstroke. Each value is the mean \pm SD of seven measurements. * $p < 0.05$. (b) ALT in plasma 60 min after the onset of heatstroke. Each value is the mean \pm SD of seven measurements. * $p < 0.05$. (c) Relationship between total Q and plasma AST. Total Q is the sum of Q_{before} and Q_{after} . (d) Relationship between total Q and plasma ALT. Hyper, the hyperthermia group; Normo, the normothermia group; Hypo, the hypothermia group.

Discussion

In the present study, we demonstrated the excessive $O_2^{\cdot-}$ generation measured in mixed venous blood and the amount of $O_2^{\cdot-}$ generation correlated well with plasma and liver MDA, HMGB1, and ICAM-1 and with plasma AST and ALT in heatstroke rats (Figures 2–7). Therefore excessive $O_2^{\cdot-}$ generation may be the primary mechanism of tissue injury and multiple organ failure in heatstroke. These findings suggest that excessive $O_2^{\cdot-}$ generation in heatstroke may enhance systemic and liver oxidative stress, endothelial activation and inflammation. Furthermore, moderate hypothermia suppressed excessive $O_2^{\cdot-}$ generation (Figures 2 and 3), systemic and liver oxidative stress (Figures 4 and 7), endothelial activation (Figure 5), and inflammatory reactions (Figure 6) in the heatstroke rats.

In the present study, excessive $O_2^{\cdot-}$ generation was detected during the induction and after the onset of heatstroke using the electrochemical sensor (Figures 2 and 3). In the pathophysiology of heatstroke, relative ischemia induced by heat exposure was considered one of the mechanisms of $O_2^{\cdot-}$ generation [3,4]. During relative tissue ischemia and hypoxia, immune cells such as neutrophils and macrophages and vascular endothelial cells might be activated and generate $O_2^{\cdot-}$ in the extracellular component [14–17]. Activated immune cells produced $O_2^{\cdot-}$ as part of

the respiratory burst via the action of membrane-bound nicotinamide adenine dinucleotide phosphate (NADPH) oxidase on molecular oxygen [18,19]. $O_2^{\cdot-}$ was also produced by the oxidation of xanthine (XAN) by xanthine oxidase (XOD), which bound to glycosaminoglycan sites in the arterial wall endothelium, and by specific NADPH oxidase in smooth muscle cells [20,21]. Among these pathways, we previously demonstrated that XOD was one of the major sources of $O_2^{\cdot-}$ generated during cerebral ischemia–reperfusion in rats [22].

In the present study, elevated MDA and ICAM-1 levels in plasma and liver were associated with $O_2^{\cdot-}$ generated in mixed venous blood in the heatstroke rats (Figures 4 and 5). Excessive $O_2^{\cdot-}$ generated in blood would produce toxic free radicals, including ONOO⁻ and OH[·], which enhanced lipid peroxidation and endothelial damage. Those were demonstrated in the present results with elevated levels of MDA and sICAM-1, respectively (Figures 4 and 5). Damaged endothelial cells might activate thrombotic and fibrinolytic responses and induced disseminated intravascular coagulation (i.e. microcirculatory ischemia–reperfusion) in heatstroke [23,24]. These reactions might create a vicious cycle as long as the core body temperature remained high and caused multiple organ failure, including the hepatocyte damage in the present study. All of these processes might relate

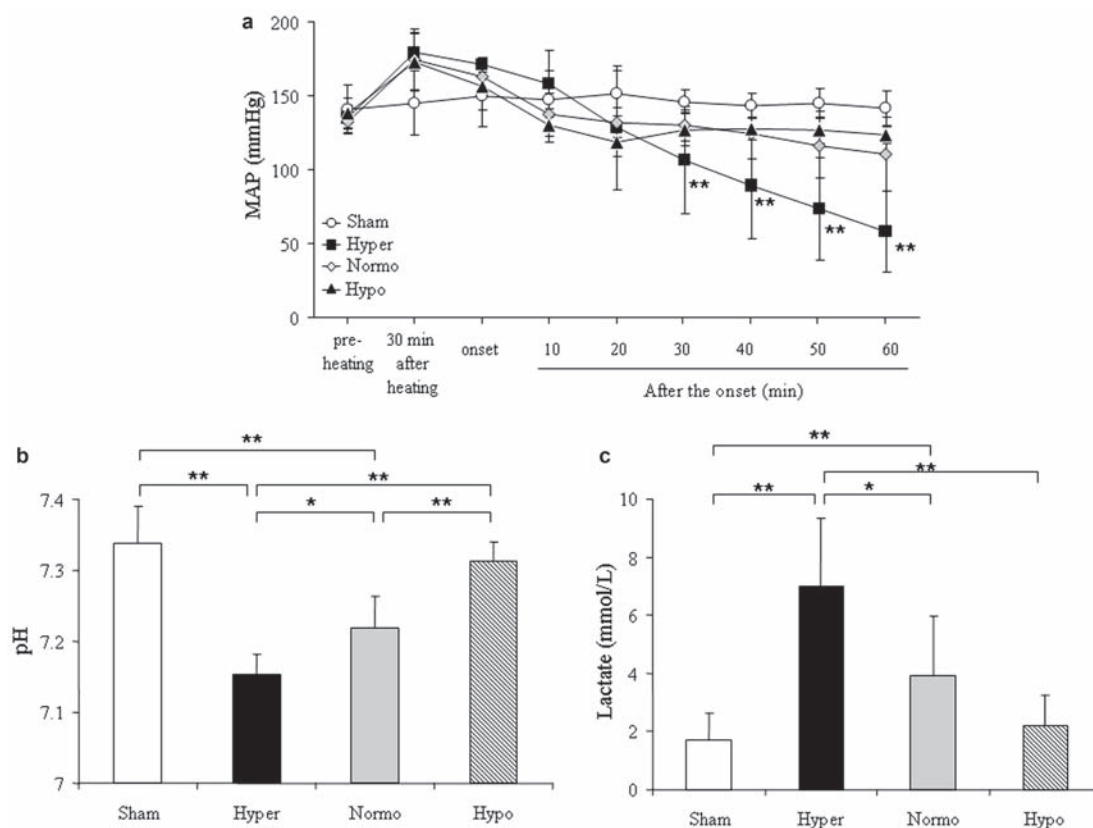


Figure 8. Mean arterial pressure (MAP), arterial pH and lactate. (a) MAP during the experiment. Each value is the mean \pm SD of seven measurements. $**p < 0.01$ for the hyperthermia group vs the sham group. (b) Arterial pH 60 min after the onset of heatstroke. Each value is the mean \pm SD of seven measurements. $*p < 0.05$, $**p < 0.01$. (c) Lactate concentration 60 min after the onset of heatstroke. Each value is the mean \pm SD of seven measurements. $*p < 0.05$, $**p < 0.01$. Hyper, the hyperthermia group; Normo, the normothermia group; Hypo, the hypothermia group.

exacerbation of systemic organ failure, at least in part, in heatstroke patients.

In the present study, elevated HMGB1 in plasma and liver was associated with O_2^- generated in mixed venous blood in the heatstroke (Figure 6). It was found that HMGB1 induced NADPH oxidase activation and ROS production in neutrophils in mice with haemorrhagic shock [25]. It was also demonstrated that correlations existed between ROS generation and HMGB1 release from hepatocytes in a rat liver ischemia–reperfusion model, from neutrophils in a mouse haemorrhagic-shock model and from macrophages and monocytes *in vitro*, respectively [25–27]. Our previous study suggested the existence of a O_2^- -mediated HMGB1 loop in the pathophysiology of global cerebral ischemia–reperfusion [13]. In the present study, elevated levels of HMGB1 in plasma and liver were associated with O_2^- generation in mixed venous blood (Figure 6), suggesting the existence of an O_2^- -mediated HMGB1 loop in the pathophysiology of heatstroke. Therefore, both O_2^- and HMGB1 might be key mediators in the pathophysiology of heatstroke.

Systemic inflammation after excessive O_2^- generation is a secondary mechanism of exacerbated tissue injury due to heatstroke. HMGB1 is ubiquitously expressed in various tissues including the liver and its

intracellular functions include stabilization of nucleosome formation and facilitation of gene transcription [28]. HMGB1 contributes to tissue injury as an early and late mediator of inflammation [29–32]. In the present study, we revealed that HMGB1 in plasma and in liver cytoplasm increased 60 min after the onset of heatstroke (Figures 6a and b). Elevation of HMGB1 in liver cytoplasm and plasma might reflect early inflammatory response to heatstroke. Furthermore, high concentrations of plasma HMGB1 might have occurred by both active and passive release from immune cells and injured organs including the liver, because HMGB1 expression in liver cytoplasm and elevated levels of plasma AST and ALT were demonstrated in the present study (Figures 6 and 7). These findings indicate that the elevation of HMGB1 in blood and organs might enhance systemic inflammation and exacerbate tissue injury, when the severity of heatstroke exceeds a certain threshold. In the present study, therapeutic moderate hypothermia after the onset of heatstroke directly suppressed mixed venous O_2^- generation, which was associated with suppression of MDA, HMGB1, ICAM-1 in plasma and liver and AST and ALT in plasma in heatstroke rats. We also demonstrated previously that moderate hypothermia suppressed jugular venous O_2^- generation in forebrain

ischemia-reperfusion rats [33]. In the pathophysiology of heatstroke, therapeutic hypothermia was reported to suppress oxidative stress and tissue injury [7,8]. Moderate hypothermia was also reported to inhibit XOD activity in a rat liver ischemia-reperfusion model and endothelial $O_2^{\cdot-}$ generation itself in focal cerebral ischemia of rats [34,35]. Furthermore, hypothermia reduced ROS formation in the perfused rat liver [36]. The results of these reports are agreeable with our present results in the hypothermia group.

There remains the concern between the reactivity of the sensor and temperature changes in heatstroke. Theoretically, temperature changes might affect the reactivity of the sensor. However, total Q of $O_2^{\cdot-}$ was well correlated with both plasma and liver MDA (Figures 4a and b). Therefore, the change of the reactivity of the sensor might be much smaller than that of the $O_2^{\cdot-}$ generation by the heatstroke in the present study.

Conclusions

We could detect excessive $O_2^{\cdot-}$ generation in the mixed venous blood in heatstroke rats. The generated $O_2^{\cdot-}$ was associated with systemic and liver oxidative stress, inflammation and endothelial activation. Moderate hypothermia was effective to prevent tissue injury by suppressing excessive $O_2^{\cdot-}$ generation. Furthermore, monitoring and evaluation of $O_2^{\cdot-}$ generation in mixed venous blood using our $O_2^{\cdot-}$ sensor would be useful for predicting tissue injury and systemic inflammation in heatstroke patients in the near future and Q might be a therapeutic target of heatstroke.

Acknowledgements

The authors thank Mrs Hitomi Ikemoto, Dr Yohei Otsuka and Dr Takahiro Yamamoto for their valuable technical assistance and Ms Masako Ueda for her patience in preparing the original manuscript.

Declaration of interest: The work described in this report was supported by a Grant-in-Aid for Young Scientists (No. 21791766) from the Ministry of Education, Science, Sports and Culture of Japan. The authors report no conflicts of interest. The authors alone are responsible for the content and writing of the paper.

References

- [1] Bouchama A, Knochel JP. Heat stroke. *N Engl J Med* 2002;346:1978–1988.
- [2] Misset B, De Jonghe B, Bastuji-Garin S, Gattolliat O, Boughrara E, Annane D, Hausfater P, Garrouste-Orgeas M, Carlet J. Mortality of patients with heatstroke admitted to intensive care units during the 2003 heat wave in France: a national multiple-center risk-factor study. *Crit Care Med* 2006;34:1087–1092.
- [3] Hall DM, Buettner GR, Oberley LW, Xu L, Matthes RD, Gisolfi CV. Mechanisms of circulatory and intestinal barrier dysfunction during whole body hyperthermia. *Am J Physiol Heart Circ Physiol* 2001;280:H509–H521.
- [4] Yang CY, Lin MT. Oxidative stress in rats with heatstroke-induced cerebral ischemia. *Stroke* 2002;33:790–794.
- [5] Lipton SA, Choi YB, Pan ZH, Lei SZ, Chen HS, Sucher NJ, Loscalzo J, Singel DJ, Stamler JS. A redox-based mechanism for the neuroprotective and neurodestructive effects of nitric oxide and related nitroso-compounds. *Nature* 1993;364:626–632.
- [6] Beckman JS, Koppenol WH. Nitric oxide, superoxide, and peroxynitrite: the good, the bad, and ugly. *Am J Physiol* 1996;271:C1424–C1437.
- [7] Hsu SF, Niu KC, Lin CL, Lin MT. Brain cooling causes attenuation of cerebral oxidative stress, systemic inflammation, activated coagulation, and tissue ischemia/injury during heatstroke. *Shock* 2006;26:210–220.
- [8] Bouchama A, Dehbi M, Chaves-Carballo E. Cooling and hemodynamic management in heatstroke: practical recommendations. *Crit Care* 2007;11:R54.
- [9] Yuasa M, Oyaizu K. Electrochemical detection and sensing of reactive oxygen species. *Curr Org Chem* 2005;9:1685–1697.
- [10] Yuasa M, Oyaizu K, Yamaguchi A, Ishikawa M, Eguchi K, Kobayashi T, Toyoda Y, Tsutsui S. Structure and redox properties of electropolymerized film obtained from iron meso-tetrakis(3-thienyl)porphyrin. *Polym Adv Technol* 2005;16:616–621.
- [11] Yuasa M, Oyaizu K, Yamaguchi A, Ishikawa M, Eguchi K, Kobayashi T, Toyoda Y, Tsutsui S. Electrochemical sensor for superoxide anion radical using polymeric iron porphyrin complexes containing axial 1-methylimidazole ligand as cytochrome c mimics. *Polym Adv Technol* 2005;16:287–292.
- [12] Fujita M, Tsuruta R, Kasaoka S, Fujimoto K, Tanaka R, Oda Y, Nanba M, Igarashi M, Yuasa M, Yoshikawa T, Maekawa T. *In vivo* real-time measurement of superoxide anion radical with a novel electrochemical sensor. *Free Radic Biol Med* 2009;47:1039–1048.
- [13] Aki HS, Fujita M, Yamashita S, Fujimoto K, Kumagai K, Tsuruta R, Kasaoka S, Aoki T, Nanba M, Murata H, Yuasa M, Maruyama I, Maekawa T. Elevation of jugular venous superoxide anion radical is associated with early inflammation, oxidative stress, and endothelial injury in forebrain ischemia-reperfusion rats. *Brain Res* 2009;1292:180–190.
- [14] Beckman JS, Beckman TW, Chen J, Marshall PA, Freeman BA. Apparent hydroxyl radical production by peroxynitrite: implications for endothelial injury from nitric oxide and superoxide. *Proc Natl Acad Sci USA* 1990;87:1620–1624.
- [15] Granger DN, Kubes P. The microcirculation and inflammation: modulation of leukocyte-endothelial cell adhesion. *J Leukoc Biol* 1994;55:662–675.
- [16] Droge W. Free radicals in the physiological control of cell function. *Physiol Rev* 2002;82:47–95.
- [17] Parks DA, Granger DN. Ischemia-induced vascular changes: role of xanthine oxidase and hydroxyl radicals. *Am J Physiol* 1983;245:G285–G289.
- [18] Guzik TJ, Korb R, Adamek-Guzik T. Nitric oxide and superoxide in inflammation and immune regulation. *J Physiol Pharmacol* 2003;54:469–487.
- [19] Babior BM, Curnutte JT, McMurrich BJ. The particulate superoxide-forming system from human neutrophils. Properties of the system and further evidence supporting its participation in the respiratory burst. *J Clin Invest* 1976;58:989–996.
- [20] Li JM, Shah AM. Endothelial cell superoxide generation: regulation and relevance for cardiovascular pathophysiology. *Am J Physiol Regul Integr Comp Physiol* 2004;287:R1014–R1030.

- [21] Rubanyi GM, Vanhoutte PM. Oxygen-derived free radicals, endothelium, and responsiveness of vascular smooth muscle. *Am J Physiol* 1986;250:H815–H821.
- [22] Ono T, Tsuruta R, Fujita M, Aki HS, Kutsuna S, Kawamura Y, Wakatsuki J, Aoki T, Kobayashi C, Kasaoka S, Maruyama I, Yuasa M, Maekawa T. Xanthine oxidase is one of the major sources of superoxide anion radicals in blood after reperfusion in rats with forebrain ischemia/reperfusion. *Brain Res* 2009;1305:158–167.
- [23] Bouchama A, Hammami MM, Haq A, Jackson J, al-Sedairy S. Evidence for endothelial cell activation/injury in heatstroke. *Crit Care Med* 1996;24:1173–1178.
- [24] Ten Cate H, Schoenmakers SH, Franco R, Timmerman JJ, Groot AP, Spek CA, Reitsma PH. Microvascular coagulopathy and disseminated intravascular coagulation. *Crit Care Med* 2001;29:S95–S98.
- [25] Tang D, Shi Y, Kang R, Li T, Xiao W, Wang H, Xiao X. Hydrogen peroxide stimulates macrophages and monocytes to actively release HMGB1. *J Leukoc Biol* 2007;81:741–747.
- [26] Tsung A, Klune JR, Zhang X, Jeyabalan G, Cao Z, Peng X, Stolz DB, Geller DA, Rosengart MR, Billiar TR. HMGB1 release induced by liver ischemia involves Toll-like receptor 4 dependent reactive oxygen species production and calcium-mediated signaling. *J Exp Med* 2007;204:2913–2923.
- [27] Fan J, Li Y, Levy RM, Fan JJ, Hackam DJ, Vodovotz Y, Yang H, Tracey KJ, Billiar TR, Wilson MA. Hemorrhagic shock induces NAD(P)H oxidase activation in neutrophils: role of HMGB1-TLR4 signaling. *J Immunol* 2007;178:6573–6580.
- [28] Bustin M. Regulation of DNA-dependent activities by the functional motifs of the high-mobility-group chromosomal proteins. *Mol Cell Biol* 1999;19:5237–5246.
- [29] Wang H, Bloom O, Zhang M, Vishnubhakat JM, Ombrellino M, Che J, Frazier A, Yang H, Ivanova S, Borovikova L, Manogue KR, Faist E, Abraham E, Andersson J, Andersson U, Molina PE, Abumrad NN, Sama A, Tracey KJ. HMG-1 as a late mediator of endotoxin lethality in mice. *Science* 1999;285:248–251.
- [30] Qiu J, Nishimura M, Wang Y, Sims JR, Qiu S, Savitz SI, Salomone S, Moskowitz MA. Early release of HMGB-1 from neurons after the onset of brain ischemia. *J Cereb Blood Flow Metab* 2008;28:927–938.
- [31] Lotze MT, Tracey KJ. High-mobility group box 1 protein (HMGB1): nuclear weapon in the immune arsenal. *Nat Rev Immunol* 2005;5:331–342.
- [32] Wang H, Yang H, Tracey KJ. Extracellular role of HMGB1 in inflammation and sepsis. *J Intern Med* 2004;255:320–331.
- [33] Koda Y, Tsuruta R, Fujita M, Miyauchi T, Kaneda K, Todani M, Aoki T, Shitara M, Izumi T, Kasaoka S, Yuasa M, Maekawa T. Moderate hypothermia suppresses jugular venous superoxide anion radical, oxidative stress, early inflammation, and endothelial injury in forebrain ischemia/reperfusion rats. *Brain Res* 2010;1311:197–205.
- [34] Hamer I, Wattiaux R, Wattiaux-De Coninck S. Deleterious effects of xanthine oxidase on rat liver endothelial cells after ischemia/reperfusion. *Biochim Biophys Acta* 1995;1269:145–152.
- [35] Maier CM, Sun GH, Cheng D, Yenari MA, Chan PH, Steinberg GK. Effects of mild hypothermia on superoxide anion production, superoxide dismutase expression, and activity following transient focal cerebral ischemia. *Neurobiol Dis* 2002;11:28–42.
- [36] Zar HA, Tanigawa K, Kim YM, Lancaster JR Jr. Mild therapeutic hypothermia for postischemic vasoconstriction in the perfused rat liver. *Anesthesiology* 1999;90:1103–1111.

This paper was first published online on Early Online on 17 February 2010.